

VERY BLUE *UV*-CONTINUUM SLOPES  $\beta$  OF LOW LUMINOSITY  $z \sim 7$  GALAXIES FROM WFC3/IR:  
EVIDENCE FOR EXTREMELY LOW METALLICITIES?<sup>1</sup>R. J. BOUWENS<sup>2,3</sup>, G. D. ILLINGWORTH<sup>2</sup>, P. A. OESCH<sup>4</sup>, M. TRENTI<sup>5</sup>, M. STIAVELLI<sup>6</sup>, C. M. CAROLLO<sup>4</sup>, M. FRANX<sup>3</sup>, P. G. VAN DOKKUM<sup>7</sup>, I. LABBÉ<sup>8</sup>, D. MAGEE<sup>2</sup>*Draft version March 21, 2019*

## ABSTRACT

We use the ultra-deep WFC3/IR data over the HUDF and the Early Release Science WFC3/IR data over the CDF-South GOODS field to quantify the broadband spectral properties of star-forming galaxies at  $z \sim 7$ . We determine the *UV*-continuum slope  $\beta$  in these galaxies, and compare the slopes with galaxies at later times to measure the evolution in  $\beta$ . For luminous  $L_{z=3}^*$  galaxies, we measure a mean *UV*-continuum slope  $\beta$  of  $-2.0 \pm 0.2$ , which is comparable to the  $\beta \sim -2$  derived at similar luminosities at  $z \sim 5 - 6$ . However, for the lower luminosity  $0.1L_{z=3}^*$  galaxies, we measure a mean  $\beta$  of  $-3.0 \pm 0.2$ . This is substantially bluer than is found for similar luminosity galaxies at  $z \sim 4$ , just 800 Myr later, and even at  $z \sim 5-6$ . In principle, the observed  $\beta$  of  $-3.0$  can be matched by a very young, dust-free stellar population, but when nebular emission is included the expected  $\beta$  becomes  $\geq -2.7$ . To produce these very blue  $\beta$ 's (i.e.,  $\beta \sim -3$ ), extremely low metallicities and mechanisms to reduce the red nebular emission are likely required. For example, a large escape fraction (i.e.,  $f_{esc} \gtrsim 0.3$ ) could minimize the contribution from this red nebular emission. If this is correct and the escape fraction in faint  $z \sim 7$  galaxies is  $\gtrsim 0.3$ , it may help to explain how galaxies reionize the universe.

*Subject headings:* galaxies: evolution — galaxies: high-redshift

## 1. INTRODUCTION

The spectral properties of high-redshift galaxies must undergo dramatic changes at some point in the past, as the metallicities in these systems drop to lower and lower values and these systems become progressively younger. In the limit of low metallicities, gas is no longer able to cool efficiently, likely resulting in massive extremely-low metallicity or Population III stars whose hot atmospheres are expected to result in a very hard *UV*-continuum spectrum and strong HeII 1640 emission. However, the strong *UV* flux coming from hot stars is expected to be largely offset by the redder nebular continuum light produced by the ionized gas surrounding these massive stars (e.g., Schaerer 2002).

The newly installed WFC3/IR camera on the Hubble Space Telescope permits us to observe faint  $z \gtrsim 7$  galaxies  $\gtrsim 40\times$  more efficiently than before, providing us with our most detailed look yet at the *UV* light and spectral properties of  $z \gtrsim 7$  galaxies. Already  $\gtrsim 25$   $z \sim 7-8$  galaxies have been identified in the early WFC3/IR data over the Hubble Ultra Deep Field (HUDF; Oesch et al. 2009b;

Bouwens et al. 2009b; McLure et al. 2009; Bunker et al. 2009), and  $\gtrsim 20$   $z \sim 7$  galaxies in the WFC3/IR Early Release Science (ERS) observations over the CDF-South (R.J. Bouwens et al. 2009, in prep).

Here we take advantage of these early WFC3/IR observations to study the spectral properties of  $z \sim 7$  galaxies. Our principal focus will be on the slope of  $z \sim 7$  galaxy spectra in the *UV*-continuum – since this slope is the principal quantity that we can derive from the available broadband imaging data with WFC3. The *UV*-continuum slope  $\beta$  ( $f_\lambda \propto \lambda^\beta$ ; e.g., Meurer et al. 1999) provides us with a powerful constraint on the age, metallicity, and dust content of high-redshift galaxies; it has already been the subject of much study at  $z \sim 3 - 6$  (Lehnert & Bremer 2003; Stanway et al. 2005; Yan et al. 2005; Bouwens et al. 2006; Hathi et al. 2008; see Bouwens et al. 2009a for a systematic study at  $z \sim 2 - 6$ ) and even at  $z \sim 7$  (Gonzalez et al. 2009) using NICMOS data.

Throughout this work, we quote results in terms of the luminosity  $L_{z=3}^*$  Steidel et al. (1999) derived at  $z \sim 3$ :  $M_{1700,AB} = -21.07$ . We refer to the HST F606W, F775W, F850LP, F105W, F125W, and F160W bands as  $V_{606}$ ,  $i_{775}$ ,  $z_{850}$ ,  $Y_{105}$ ,  $J_{125}$ , and  $H_{160}$ , respectively, for simplicity. Where necessary, we assume  $\Omega_0 = 0.3$ ,  $\Omega_\Lambda = 0.7$ ,  $H_0 = 70$  km/s/Mpc. All magnitudes are in the AB system (Oke & Gunn 1983).

## 2. OBSERVATIONAL DATA

Our primary dataset for this analysis is the ultra deep WFC3/IR data over the HUDF and the wide-area WFC3/IR ERS observations over the CDF-South (PI O'Connell: GO 11359). The HUDF data permit us to both identify lower luminosity  $z \sim 7$  galaxies and quantify their properties (e.g., Oesch et al. 2009b), while the ERS data permit us to do the same for more luminous  $z \sim 7$  galaxies.

For our HUDF dropout selections, we make use of the

<sup>1</sup> Based on observations made with the NASA/ESA Hubble Space Telescope, which is operated by the Association of Universities for Research in Astronomy, Inc., under NASA contract NAS 5-26555. These observations are associated with programs #11563, 9797.

<sup>2</sup> UCO/Lick Observatory, University of California, Santa Cruz, CA 95064

<sup>3</sup> Leiden Observatory, Leiden University, NL-2300 RA Leiden, Netherlands

<sup>4</sup> Institute for Astronomy, ETH Zurich, 8092 Zurich, Switzerland; poesch@phys.ethz.ch

<sup>5</sup> University of Colorado, Center for Astrophysics and Space Astronomy, 389-UCB, Boulder, CO 80309, USA

<sup>6</sup> Space Telescope Science Institute, Baltimore, MD 21218, United States

<sup>7</sup> Department of Astronomy, Yale University, New Haven, CT 06520

<sup>8</sup> Carnegie Observatories, Pasadena, CA 91101, Hubble Fellow

v1.0 reductions of the HUDF ACS data (Beckwith et al. 2006) rebinned on a  $0.06''$ -pixel scale, and our own reduction of the HUDF09 WFC3/IR data over the HUDF (Bouwens et al. 2009b; Oesch et al. 2009b). The optical ACS imaging over the HUDF reach to 29.4, 29.8, 29.7, and 29.0 AB mag ( $5\sigma$ :  $0.35''$ -diameter apertures) in the  $B_{435}$ ,  $V_{606}$ ,  $i_{775}$ ,  $z_{850}$  bands, respectively, while the near-IR WFC3/IR data reach to 28.8, 28.8, and 28.7 ( $5\sigma$ :  $0.35''$  apertures) in the  $Y_{105}$ ,  $J_{125}$ , and  $H_{160}$  bands, respectively. The FWHM of the PSFs are  $\sim 0.10''$  for the ACS data and  $\sim 0.16''$  for the WFC3/IR data.

For our dropout selections over the WFC3/IR ERS fields, we make use of our own reductions of the available ACS/WFC data over the GOODS fields (Bouwens et al. 2006; Bouwens et al. 2007). Our reductions reach to 28.0, 28.2, 27.5, and 27.4 in the  $B_{435}$ ,  $V_{606}$ ,  $i_{775}$ ,  $z_{850}$ , respectively ( $5\sigma$ :  $0.35''$  apertures). This is similar to the GOODS v2.0 reductions, but reach  $\sim 0.1$ - $0.3$  mag deeper in the  $z_{850}$ -band due to the inclusion of all the SNe follow-up data (Riess et al. 2007). Our reduction of the WFC3/IR ERS data was performed using the same procedures as we used on the HUDF09 WFC3/IR data. These data reach to 27.7 and 27.4 in the  $J_{125}$  and  $H_{160}$  bands, respectively ( $5\sigma$ :  $0.35''$  apertures).

### 3. RESULTS

(a) *Catalog Creation*: Our procedure for source detection and photometry is similar to that used in previous studies by our team (e.g., Bouwens et al. 2007; Bouwens et al. 2009a) and relies upon the SExtractor software (Bertin & Arnouts 1996) run in double image mode. Source detection is performed off the square root of  $\chi^2$  image (Szalay et al. 1999: similar to a coadded image) constructed from all images redward of the Lyman break. Colors are measured in small scalable apertures with a Kron (1980) parameter of 1.5 (typically  $\sim 0.4''$ -diameter apertures). Fluxes measured in these small scalable apertures are then corrected (typically by  $\sim 0.4$  mag) to total magnitudes using the additional flux in a larger scalable aperture (Kron parameter of 2.5).

(b)  *$z \sim 7$   $z$ -dropout selection*: For our  $z \sim 7$   $z$ -dropout selection, we use a criterion very similar that used by Oesch et al. (2009b) over the HUDF09 WFC3/IR field:

$$(z_{850} - Y_{105} > 0.8) \wedge (Y_{105} - J_{125} < 0.8)$$

for our lower luminosity  $z$ -dropout sample. Over the WFC3/IR ERS fields, no deep WFC3  $Y_{105}$ -band coverage is available, so we make use of the following criterion (R.J. Bouwens 2009, in prep):

$$(z_{850} - J_{125} > 0.8) \wedge (J_{125} - H_{160} < 0.3)$$

Sources are required to be undetected ( $< 2\sigma$ ) in all bands blueward of the break to ensure that our selections are largely free of lower redshift contaminants. We also require that each selected source not be detected at  $> 1.5\sigma$  in more than one band blueward of the break. Sources must be detected at  $> 5.5\sigma$  in a band redward of the break to ensure that sources in our selection are real and do not correspond to spurious detections.

(c) *UV-continuum slope Measurements*: The UV-continuum slopes  $\beta$  we estimate for sources in our  $z \sim 7$   $z$ -dropout sample are derived from the broadband color

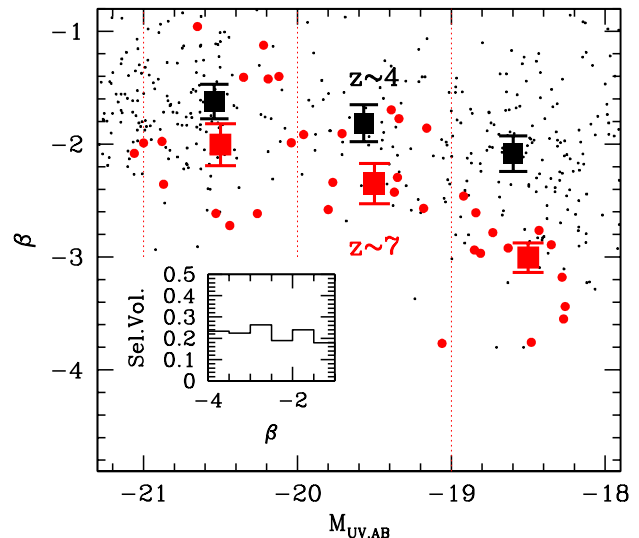


FIG. 1.— UV-continuum slope  $\beta$  versus absolute UV magnitude. The red circles show the  $\beta$  determinations and absolute magnitudes (derived from the  $J_{125} - H_{160}$  colors and  $(J_{125} + H_{160})_{AB}$  magnitude, respectively) for individual  $z \sim 7$  galaxies in our HUDF09 and ERS selections. The large red squares (with  $1\sigma$  error bars) represent the mean values in 1-mag bins (dotted lines). The black points correspond to the  $\beta$  determinations at  $z \sim 4$  (Bouwens et al. 2009a). The  $\beta$ 's for lower luminosity galaxies at  $z \sim 7$  (red circles) are much bluer (by  $\Delta\beta$  of  $\sim 1$ ) than those derived at  $z \sim 4$  (a  $4\sigma$  difference). (inset) The relative volumes available for selecting galaxies with various  $\beta$ 's using our HUDF09  $z$ -dropout criterion (see §3d). These volumes do not depend significantly on  $\beta$ , showing that the blue  $\beta$ 's observed for faint  $z \sim 7$  galaxies is not a selection effect.

$J_{125} - H_{160}$  as

$$\beta = 4.29(J_{125} - H_{160}) - 2.00 \quad (1)$$

The  $J_{125}$  and  $H_{160}$  bands here probe rest-frame  $\sim 1550\text{\AA}$  and  $\sim 1940\text{\AA}$ , respectively, for the typical  $z \sim 7$   $z$ -dropout in our sample, and are not affected by Ly $\alpha$  emission or IGM absorption (in contrast to the  $Y_{105}$ -band).

In Figure 1, we show the  $\beta$  determinations for  $z \sim 7$   $z$ -dropouts versus luminosity. Both our ultra-deep HUDF09 and wide-area ERS selections are included, as is the  $z \sim 4$  data from Bouwens et al. (2009a). The trend of  $\beta$  with luminosity is clearly illustrated with the large squares. The difference between  $z \sim 7$  and  $z \sim 4$  is striking.

(d) *Consideration of Possible Selection Biases*: The distribution of UV-continuum slopes  $\beta$  we derive for galaxies in our  $z \sim 7$   $z$ -dropout can be affected by the selection process. This effect is seen in lower redshift samples, where galaxies with bluer  $\beta$ 's have a larger selection volume than galaxies with redder  $\beta$ 's. To determine the importance of such effects, we constructed models with various  $\beta$  distributions, added galaxies with these distributions to the observational data, and then attempted to reselect these galaxies using the selection criteria in §3(b) to estimate the effective selection volume versus  $\beta$ . We modelled the pixel-by-pixel profiles of the sources using similar luminosity  $z \sim 4$   $B$ -dropouts from the Bouwens et al. (2007) HUDF sample, but scaled in size (physical) as  $(1+z)^{-1}$  to match the observed size-redshift relationship (Oesch et al. 2009c; see also Ferguson et al. 2004; Bouwens et al. 2004).

The selection volumes derived from these simulations

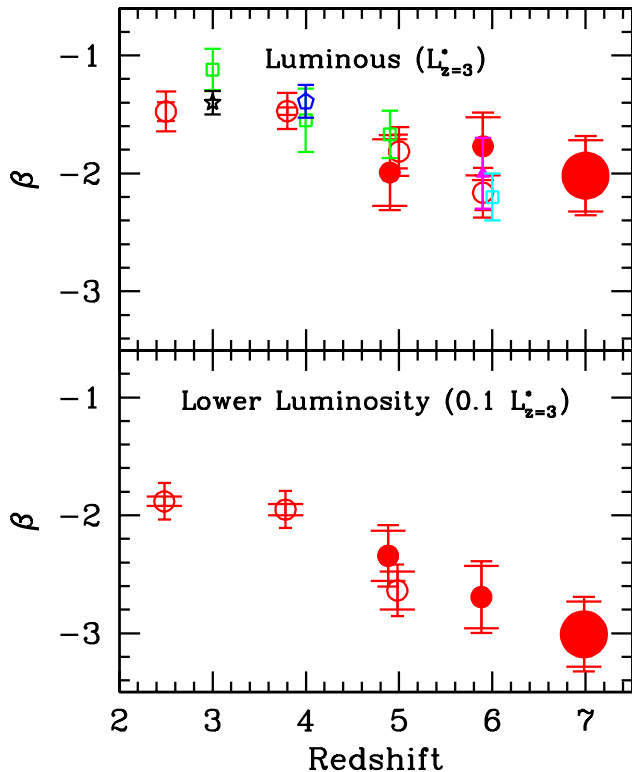


FIG. 2.— Mean  $UV$ -continuum slope measured for galaxies at  $z \sim 7$  (large red circles) versus galaxies of similar luminosities at lower redshifts. The top panel shows the evolution in this slope for galaxies with a  $UV$  luminosity of  $L^*_{z=3}$  ( $-21$  AB mag) and the bottom panel shows the evolution for galaxies with a  $UV$  luminosity of  $0.1L^*_{z=3}$  ( $-18.5$  AB mag). The determinations of Bouwens et al. (2009a) based upon ACS+NICMOS data are shown with the open red circles. The short error bars show the random errors while the longer error bars also account for possible systematic errors (e.g., see Bouwens et al. 2009a). We also show  $\beta$  determinations by Stanway et al. (2005: *cyan square*), Ouchi et al. (2004: *blue pentagon*), Adelberger & Steidel (2000: *black star*), and Hathi et al. (2008: *green open squares*). Note the dramatic change in  $\beta$  in the  $\sim 800$  Myr from  $z \sim 7$  to  $z \sim 4$  for lower luminosity galaxies.

are shown in the inset to Figure 1. Encouragingly, these volumes show only a modest dependence upon the input  $\beta$  for the range  $-4 < \beta < -1$ , and so selection biases should be minimal.

(e) *Low-redshift Comparison Samples:* To interpret the  $\beta$ 's we derive from our  $z \sim 7$   $z$ -dropout selections, it is useful to compare them with the  $\beta$ 's found for similar luminosity galaxies at  $z \sim 4 - 6$ . Bouwens et al. (2009a) provide determinations of these slopes as a function of luminosity at  $z \sim 2 - 6$ . The  $UV$ -continuum slope measurements at  $z \sim 4$  are also shown in Figure 1 for comparison.

We can take advantage of the very deep, high-quality WFC3/IR data to obtain self-consistent determinations of these slopes at  $z \sim 5-6$ . The  $z \sim 5$   $V$  and  $z \sim 6$   $i$ -dropouts over the HUDF and GOODS ERS data are selected in the same way as in Bouwens et al. (2007: see also Giavalisco et al. 2004; Beckwith et al. 2006), except that at  $z \sim 6$  we also require galaxies to satisfy the criterion ( $z_{850} - J_{125} < 0.6$ ). At  $z \sim 5$  and  $z \sim 6$ , the  $\beta$ 's are estimated based upon the  $z_{850} - (Y_{105} + J_{125})/2$  and  $Y_{105} - (2J_{125} + H_{160})/3$  colors, respectively, which are a good match in rest-frame wavelength to the  $J_{125} - H_{160}$  colors used to estimate  $\beta$  at  $z \sim 7$ . The conversion for-

mulas we use are

$$\beta = 4.07(z_{850} - (Y_{105} + J_{125})/2) - 2.00 \quad (z \sim 5) \quad (2)$$

$$\beta = 3.78(Y_{105} - (2J_{125} + H_{160})/3) - 2.00 \quad (z \sim 6) \quad (3)$$

In Figure 2, we plot these  $\beta$  determinations as a function of redshift, for both luminous  $L^*$  galaxies and lower luminosity galaxies.

(f)  *$z \sim 8$  Comparison Sample:* Faint  $z \sim 8$   $Y_{105}$ -dropout candidates in the HUDF09 WFC3/IR data (Bouwens et al. 2009b) also have very blue  $J_{125} - H_{160}$  colors, again suggesting  $\beta$ 's of  $\sim -3$ . We decided not to consider this sample here because the  $J_{125}$  band can be affected by Lyman series absorption and Ly $\alpha$  emission at  $z > 8.1$ , and hence the results would be less robust.

#### 4. DISCUSSION

Before discussing the extraordinarily blue  $UV$ -continuum slopes  $\beta \sim -3$  found for lower luminosity galaxies at  $z \sim 7$ , we first consider the relatively luminous  $L^*_{z=3}$  galaxies. These sources have measured  $\beta$ 's of  $-2$ , which is very similar to that observed for luminous galaxies at  $z \sim 3 - 6$  (Figure 2). Such slopes can be fit by a moderately young, subsolar ( $0.2 Z_{\odot}$ ) stellar population, with a maximum  $E(B - V)$  of  $\sim 0.05$  (Calzetti et al. 2000 extinction law: see also Bouwens et al. 2009a).

The lower luminosity ( $0.1L^*_{z=3}$ , or  $-18.5$  AB mag) galaxies at  $z \sim 7$ , by contrast, have observed  $\beta$ 's of  $-3.0 \pm 0.2$ . This is much bluer than for luminous  $z \sim 7$  galaxies (by  $\Delta\beta \sim 1$ ) and also much bluer than is found at  $z \sim 5 - 6$  (Figures 1-2). This makes these galaxies of great interest since they are likely to be even younger, more metal poor, and dust-free than any galaxies known.

This is not a selection effect (§3d), and cannot be attributed to Ly $\alpha$  emission contributing to the broadband fluxes for  $z \sim 7$   $z$ -dropouts in our samples. Ly $\alpha$  does not move into the  $J_{125}$ -band (used to estimate  $\beta$ ) until  $z \gtrsim 8.1$ , and  $\lesssim 10\%$  of our  $z$ -dropout sample extends to  $z > 8$ .

What then is the explanation for the very blue  $UV$ -continuum slopes  $\beta$ ? We explore several possibilities:

(a) *Standard stellar population models:* A first question is whether it is possible to obtain a  $\beta$  of  $\sim -3$  using standard stellar population models (e.g., Leitherer et al. 1999; Bruzual & Charlot 2003). The answer is that it is possible, but only for very young ( $< 5$  Myr) star-forming systems (see Figure 3). However, to do so ignores the nebular continuum emission that would come from the ionized gas around the young stars. Including this nebular continuum emission to the total light can redden the observed  $\beta$  by as much as  $\Delta\beta \sim 0.5$ .

Figure 3 also shows the  $UV$ -continuum slopes  $\beta$  predicted for several low metallicity ( $0.02 Z_{\odot}$  and  $0.2 Z_{\odot}$ ) starbursts, as a function of age for the Schaerer (2002; 2003) stellar population models (which – like *Starburst99* Leitherer et al. 1999 – include a nebular contribution). In the best cases, the models predict  $UV$ -continuum slopes as blue as  $-2.7$ , which is redder than what we observe in our samples. This suggests that lower metallicities are needed since the standard Leitherer et al. (1999) or Bruzual & Charlot (2003) stellar population models simply do not produce blue enough colors to match those found in our lower luminosity  $z \sim 7$  sample.

(b) *Extremely low metallicities ( $\leq 10^{-3} Z_{\odot}$ ):* In Figure 4 we present the  $\beta$ 's predicted by the Schaerer (2003)

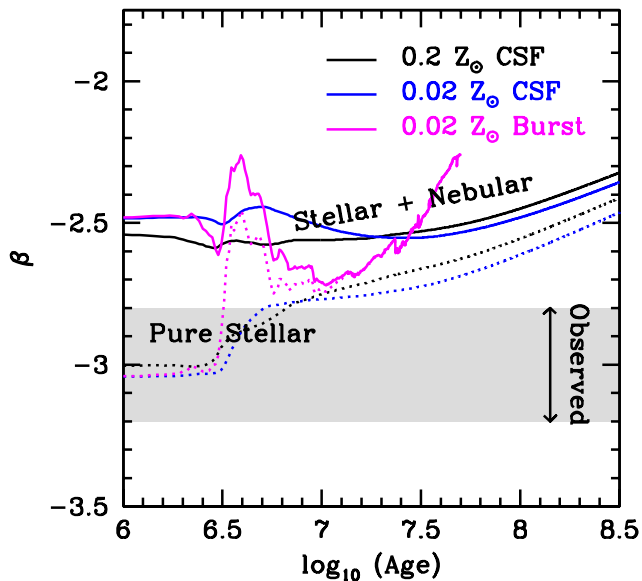


FIG. 3.— UV-continuum slope  $\beta$  we would expect for  $z \sim 7$  galaxies as a function of age for constant star formation (CSF) models and an instantaneous burst (Schaerer 2002). The gray band denotes the observed mean  $\beta$  and its uncertainty. The slopes  $\beta$  derived from the stellar light (dotted lines) and the stellar + nebular light (solid lines) are shown. While it is in principle possible to obtain  $\beta$ 's of  $-3$  with standard low metallicity ( $\geq 0.02 Z_{\odot}$ ) models, including the nebular emission associated with hot stars make the predicted  $\beta$ 's  $\geq -2.7$  and hence too red.

stellar population models (which conveniently provide predictions at extremely low metallicities) as a function of age for instantaneous bursts assuming a metallicity of  $0.5 \times 10^{-3} Z_{\odot}$ ,  $0.5 \times 10^{-5} Z_{\odot}$ , and zero (population III).<sup>9</sup> From the figure, it is clear that the nebular component contributes a significant fraction of the total UV light output from  $\lesssim 10^{-3} Z_{\odot}$  stellar populations.

While initially somewhat red due to the nebular contribution, the predicted  $\beta$ 's for these ultra-low metallicity models become much bluer at ages  $> 10$  Myr, eventually reaching  $\beta$ 's of  $-3$ . Such metallicities and ages are not necessarily unreasonable for lower luminosity galaxies at  $z \sim 7$ , and therefore at least one possible explanation for the very blue  $\beta$ 's in our selections is that the metallicities for galaxies in our sample may be  $\lesssim 10^{-3} Z_{\odot}$ .

The above explanation may explain some of the very blue galaxies in our selection, but given that  $\beta \sim -3$  only for a very limited period (10-30 Myr after a burst), it seems unlikely to be the general explanation (unless updated models revise the theoretical SEDs).

(c) *Top-heavy IMF*: One seemingly attractive explanation for the very blue  $\beta$ 's observed is through a top-heavy IMF, since galaxy stellar populations would be weighted towards very massive, blue stars. The difficulty with this explanation is these same massive stars are extraordinarily efficient at ionizing the gas around them – resulting in substantial nebular continuum emission and leaving the galaxy with a net  $\beta$  no bluer (and likely redder) than the young ( $< 1$  Myr) bursts shown in Figures 3-4 (see also discussion in Leitherer & Heckman 1995).

(d) *Minimizing nebular emission*: A significant obsta-

<sup>9</sup> The use of instantaneous burst models allows us to explore the most extreme cases – all other models  $\tau$ , inverse  $\tau$ , CSF will produce comparable  $\beta$ 's.

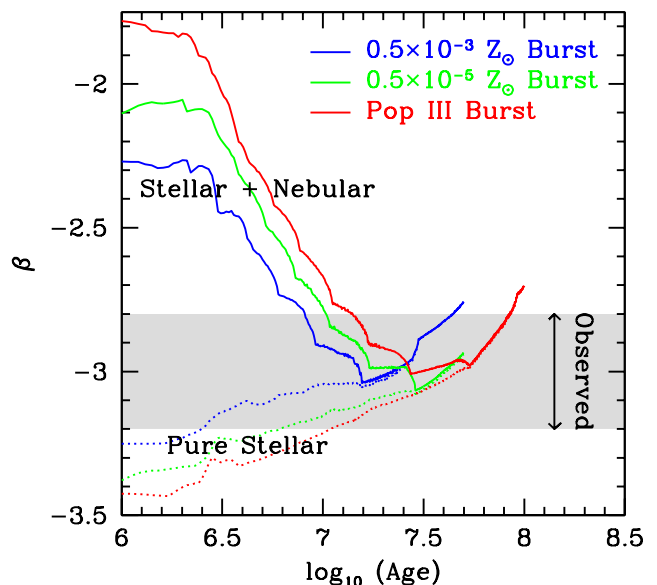


FIG. 4.— UV-continuum slope  $\beta$  Schaerer (2003) calculated as a function of age for instantaneous burst models for different metallicities. Both the slopes  $\beta$  derived from the stellar light (dotted lines) and the stellar + nebular light (solid lines) are shown. The pure stellar light (dotted lines) has very blue UV-continuum slopes  $\beta$ 's ( $\beta \lesssim -3$ ) for all the low metallicity cases considered here. Changing the IMF does not appear to change the conclusion here in any significant way. Of course, these same very hot low metallicity stars also ionize the gas around them, thus producing a substantial amount of redder nebular continuum light. This makes the total SED of a galaxy much redder in general, and in the calculations by Schaerer (2003) shown here,  $\beta$  never becomes bluer than  $-3.0$ .

cle to matching the very blue  $\beta$ 's observed is the red nebular emission associated with hot, ionizing stars. The nebular contribution could be reduced in lower luminosity galaxies in a number of ways, by changes to the ionization parameter, metallicity, geometry, etc. Assessing the impact of such changes would benefit from further detailed modelling. However, we should emphasize that regardless of any changes to the nebular contribution very low metallicity models appear to be needed to match the very blue  $\beta$ 's observed.

(e) *Changes in Escape Fraction?*: One possibility that we have explored to effectively reduce the nebular emission contribution is if the ionizing radiation leaks directly into the IGM (e.g., due to the effect of SNe on the galaxies' ISM, possibly from a top-heavy IMF: Trenti & Shull 2009). We consider such a possibility schematically in Figure 5, showing the time-averaged  $\beta$ 's we would expect for stellar populations of various metallicities as a function of the escape fraction  $f_{esc}$  of ionizing photons into the IGM. For escape fractions of unity, we would simply recover the  $\beta$ 's from the pure stellar SEDs and for escape fractions of zero, we recover the stellar + nebular SEDs. For fractional  $f_{esc}$ , we interpolate between these two extremes. We compute these time-averaged  $\beta$ 's by averaging over the  $\beta$ 's predicted in Figure 4 for the pure stellar component and for the stellar+nebular component.

The mean  $\beta$  observed is shown in Figure 5 as the gray shaded region. Comparing the predicted  $\beta$ 's with the observations, we see that escape fractions  $f_{esc} \gtrsim 0.3$  would permit us to easily match the blue  $\beta$ 's observed. Such an



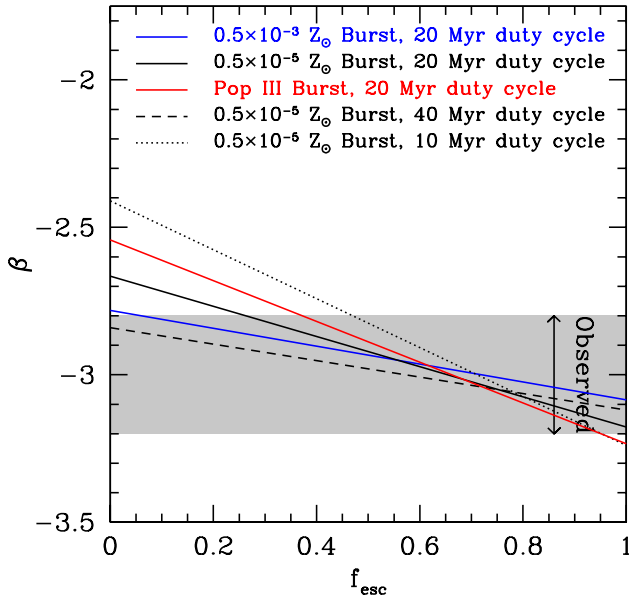


FIG. 5.— Mean UV-continuum slopes  $\beta$ 's predicted for high-redshift galaxy samples versus the escape fraction. The predictions are made using the Schaerer (2003) stellar population models (including nebular emission) for metallicities of  $< 10^{-3} Z_{\odot}$ . Galaxies are assumed to be observed at some random point during their star formation histories and to experience instantaneous bursts of star formation every 10-40 Myr (the dashed, solid, and dotted lines give the average  $\beta$  for the first 10, 20, and 40 Myr, respectively, of the instantaneous burst). For escape fractions of unity, all of the ionizing radiation from a galaxy escapes into the IGM and hence does not contribute to ionizing the gas within a galaxy (and hence the contribution from nebular continuum emission to the total light is minimal). On the other hand, for escape fractions of zero (preferred in some simulations: e.g., Gnedin et al. 2008), the ionizing radiation from the hot stars does not make it out of galaxies – resulting in substantial nebular continuum emission (see Figure 4) and hence a much redder  $\beta$ . Perhaps the very blue  $\beta$ 's observed (shaded gray region) could indicate that the escape fraction is larger at  $f_{\text{esc}} \gtrsim 0.3$  than what has commonly been considered to date?

escape fraction is significantly higher than the  $\sim 10\%$  frequently assumed in calculations assessing the sufficiency of the observed population of galaxies to reionize the universe. Since most of the luminosity density at  $z > 7$  comes from low luminosity galaxies, the estimated number of ionizing photons in the  $z > 7$  universe could increase by factors of  $\gtrsim 3$ . Such a large change could provide the needed photons to reionize the universe, providing a resolution to the current debate (see, e.g., Bouwens et al. 2008; Oesch et al. 2009b; McLure et al. 2009; Bunker et al. 2009; Gonzalez et al. 2009; Ouchi et al. 2009; Pawlik et al. 2009).

**Summary:** The strikingly blue UV-continuum slopes  $\beta$ 's seen at lower luminosities at  $z \sim 7$  (also apparent in the Bouwens et al. 2009b  $z \sim 8$  sample) indicate that we are now beginning to explore a regime where the nature of galaxies and their stellar populations are undergoing a dramatic change. These results raise many as yet unanswered questions, but could be heralding the transition from the first stars and youngest objects within the first 400 Myr at  $z \gtrsim 10$  to the types of galaxies that dominate the universe for the next 2 Gyr and provide clues as to the source of photons that reionize the universe.

We thank Daniel Schaerer for helpful conversations. We are grateful to all those at NASA, STScI and throughout the community who have worked so diligently to make Hubble the remarkable observatory that it is today. We acknowledge the support of NASA grant NAG5-7697 and NASA grant HST-GO-11563.01.

## REFERENCES

- Beckwith, S. V. W., et al. 2006, *AJ*, 132, 1729  
 Bertin, E. and Arnouts, S. 1996, *A&AS*, 117, 39  
 Bouwens, R. J., Illingworth, G. D., Blakeslee, J. P., Broadhurst, T. J., & Franx, M. 2004, *ApJ*, 611, L1  
 Bouwens, R.J., Illingworth, G.D., Blakeslee, J.P., & Franx, M. 2006, *ApJ*, 653, 53  
 Bouwens, R. J., Illingworth, G. D., Franx, M., & Ford, H. 2007, *ApJ*, 670, 928  
 Bouwens, R.J., et al. 2009a, *ApJ*, in press, arXiv:0909.4074  
 Bouwens, R.J., et al. 2009b, *ApJ*, submitted, arXiv:0909.1803  
 Bruzual, G., & Charlot, S. 2003, *MNRAS*, 344, 1000  
 Bunker, A., et al. 2009, *MNRAS*, submitted, arXiv:0909.2255  
 Calzetti, D., Armus, L., Bohlin, R. C., Kinney, A. L., Koornneef, J., & Storchi-Bergmann, T. 2000, *ApJ*, 533, 682  
 Ferguson, H. C. et al. 2004, *ApJ*, 600, L107  
 Giavalisco, M., et al. 2004a, *ApJ*, 600, L93  
 Gnedin, N. Y., Kravtsov, A. V., & Chen, H.-W. 2008, *ApJ*, 672, 765  
 Gonzalez, V., Labbe, I., Bouwens, R., Illingworth, G., Franx, M., Kriek, M., Brammer, G. 2009, *ApJ*, submitted, arXiv:0909.3517  
 Hathi, N. P., Malhotra, S., & Rhoads, J. E. 2008, *ApJ*, 673, 686  
 Kron, R. G. 1980, *ApJS*, 43, 305  
 Lehnert, M. D. & Bremer, M. 2003, *ApJ*, 593, 630  
 Leitherer, C., & Heckman, T. M. 1995, *ApJS*, 96, 9  
 Leitherer, C., et al. 1999, *ApJS*, 123, 3  
 McLure, R., et al. 2009, *MNRAS*, submitted, arXiv:0909.2437  
 Meurer, G. R., Heckman, T. M., & Calzetti, D. 1999, *ApJ*, 521, 64  
 Oesch, P. A., et al. 2009a, *ApJ*, 690, 1350  
 Oesch, P.A., et al. 2009b, *ApJ*, submitted, arXiv:0909.1806  
 Oesch, P.A., et al. 2009c, *ApJ*, submitted, arXiv:0909.5183  
 Oke, J. B., & Gunn, J. E. 1983, *ApJ*, 266, 713  
 Ouchi, M., et al. 2004, *ApJ*, 611, 660  
 Ouchi, M., et al. 2009, arXiv:0908.3191  
 Pawlik, A. H., Schaye, J., & van Scherpenzeel, E. 2009, *MNRAS*, 394, 1812  
 Riess, A. G., et al. 2007, *ApJ*, 659, 98  
 Schaerer, D. 2002, *A&A*, 382, 28  
 Schaerer, D. 2003, *A&A*, 397, 527  
 Stanway, E. R., McMahon, R. G., & Bunker, A. J. 2005, *MNRAS*, 359, 1184  
 Steidel, C. C., Adelberger, K. L., Giavalisco, M., Dickinson, M., and Pettini, M. 1999, *ApJ*, 519, 1  
 Szalay, A. S., Connolly, A. J., & Szokoly, G. P. 1999, *AJ*, 117, 68  
 Trenti, M., & Shull, M. 2009, arXiv:0905.4505  
 Yan, H., et al. 2005, *ApJ*, 634, 109